Prevalence of the thioamide $\{\cdots H–N–C=S\}_2$ synthon—solid-state (X-ray crystallography), solution (NMR) and gas-phase (theoretical) structures of *O*-methyl-*N*-aryl-thiocarbamides

Soo Yei Ho,[a] Ryan P. A. Bettens,[a] Dainis Dakternieks,*[b] Andrew Duthie[b] and Edward R. T. Tiekink*[c]

Received 7th October 2005, Accepted 16th November 2005
First published as an Advance Article on the web 23rd November 2005
DOI: 10.1039/b514254g

Structural investigations, *i.e.* solid-state (X-ray), solution (^{1}H NMR) and gas-phase (theoretical), on molecules with the general formula MeOC(=S)N(H)C_6H_4-4-Y: Y = H (**1**), NO_2 (**2**), C(=O)Me (**3**), Cl (**4**) have shown a general preference for the adoption of an *E*-conformation about the central C–N bond. Such a conformation allows for the formation of a dimeric hydrogen-bonded $\{\cdots H–N–C=S\}_2$ synthon as the building block. In the cases of **1**–**3**, additional C–H···O interactions give rise to the formation of tapes of varying topology. A theoretical analysis shows that the preference for the *E*-conformation is about the same as the crystal packing stabilisation energy and consistent with this, the compound with Y = C(=O)OMe, (**5**), adopts a *Z*-conformation in the solid-state that facilitates the formation of N–H···O, C–H···O and C–H···S interactions, leading to a layer structure. Global crystal packing considerations are shown to be imperative in dictating the conformational form of molecules **1**–**5**.

Introduction

In the ideal situation crystal engineers require synthons that form consistently and are sufficiently directional to allow for supramolecular control and therefore, the rational design of crystal structures. Of the gamut of intermolecular forces available, arguably the most reliable are hydrogen-bonding interactions that are formed typically but not exclusively between hydrogen atoms bound to electronegative elements such as oxygen and nitrogen, and electronegative acceptors such as, again, oxygen and nitrogen. If one were asked to name a reliable synthon based on hydrogen-bonding interactions, perhaps the carboxylic acid dimer, $\{\cdots H–O–C=O\}_2$, with an eight-membered $R_2^2(8)$ ring,[1] would immediately come to mind. While this synthon can be and has been used to good effect in the context of crystal engineering, in both the realms of organic and coordination chemistry, not all is as it should be. A systematic survey of organic molecules containing the carboxylic acid functionality showed that it was in only approximately one-third of their solid-state structures where the carboxylic acid dimer was formed.[2] This observation can be largely, but not exclusively, explained in terms of competing sites for intermolecular interactions. The related amide $R_2^2(8)$ synthon, $\{\cdots H–N–C=O\}_2$, is observed in only approximately 16% of structures where there are no competing groups, a result that may reflect the tendency of such residues to associate to form molecular tapes.[2] In this context, the focus of this contribution is directed towards the analogous thioamide synthon, in particular to the prevalence of the $\{\cdots H–N–C=S\}_2$ dimer synthon in force in structures of the general formula ROC(=S)N(H)R′, where R = alkyl and aryl; Chart 1.

Ligands based on ROC(=S)N(H)R′, both in the neutral and, in particular, deprotonated forms, exhibit an interesting range of coordination modes. Briefly, and for example, the neutral molecule functions as a monodentate thione in the structures of *trans*-Pd[S=C(OEt)N(H)Me]$_2$(SCN)$_2$[3] and [Au(S=C(OEt)-N(H)Me]$_2$Cl.[4] In the structure of Pd[S=C(OMe)N(H)-$CH_2CH=CH_2$]Cl_2, the thiocarbamide functions as a chelating ligand by forming interactions to palladium *via* the thione sulfur atom and the allyl group.[5] Deprotonated forms of ROC(=S)N(H)R′ have been observed to function as a monodentate thiolate, *e.g.* Ph_3PAu[SC(OMe)N=Ph],[6] but more commonly as a S-, N- chelate, *e.g.* Re(O)(PPh$_3$)[SC(OEt)=NC_6H_4-4-Me]Cl_2[7] and Tc(N)(PPh$_3$)[SC(OEt)=NPh]Cl.[8] A bidentate S-, N-bridging mode is found in the structure of dinuclear $\{$Cu[P(OMe)$_3$][SC(OC_6H_2-2,6-Bu$_2$-4-Me)=NPh]$\}_2$[9] and, finally, a μ_3-coordination mode in which the sulfur atom bridges two copper atoms and nitrogen links a third copper atom is found in several copper complexes as exemplified in the hexanuclear structure of $\{$Cu[SC(OC_6H_4-4-Me)=NPh]$\}_6$.[10] Such a range of coordination modes and geometries has resulted in several studies being conducted on the structural chemistry of the thiocarbamide molecules themselves.

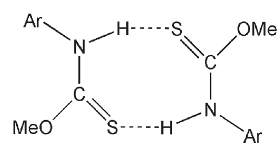

I

Chart 1 Thioamide $\{\cdots H–N–C=S\}_2$ dimer synthon.

[a]Department of Chemistry, National University of Singapore, Singapore 117543
[b]Centre for Chiral and Molecular Technologies, Deakin University, Geelong, Victoria 3217, Australia. E-mail: dainis@deakin.edu.au; Fax: 61 3 5227 1040; Tel: 61 3 5227 1318
[c]Department of Chemistry, The University of Texas at San Antonio, San Antonio, Texas 78249-0698, USA. E-mail: Edward.Tiekink@utsa.edu; Fax: 1 210 458 7428; Tel: 1 210 458 5774

In the seven known X-ray crystal structures of molecules of the general formula ROC(=S)N(H)R′, where R, R′ = alkyl and/or aryl, a whole variety of intermolecular interactions are observed. In the 'simple' derivatives, *i.e.* with no additional substitution in the aryl or alkyl groups, namely MeOC(=S)N(H)Ph,[11] EtOC(=S)N(H)Ph,[12] and (C_6H_3-2,6-Me_2)OC(=S)N(H)Ph,[13] molecules associate into dimers *via* the $R_2^2(8)$ synthon, {···H–N–C=S}$_2$; as represented in Chart 1. This association is facilitated by an *E*-conformation about the central C–N bond that comes about owing to significant intramolecular hydrogen bonding (**II**, Chart 2) and resonance structures (**III**, Chart 2), which restrict rotation about this bond. A similar *E*-conformation is found in the structure of iPrOC(=S)N(H)R′, where R′ is 2-furoyl.[14] However, in this case the {···H–N–C=S}$_2$ synthon is not observed owing to the presence of intramolecular N–H···O and C–H···S bonds. Similarly, in the structures of ROC(=S)N(H)R′, where R = Me and Et, and R′ is 2,3,4,6-tetra-*O*-acetyl-β-D-glucopyranosyl,[15] and MeOC(=S)N(H)R′, where R′ is 2-(2-methyl-5-nitro-1H-imidazol-1-yl),[16] the {RC(=S)N(R)H)}$_2$ synthon is absent owing to the presence of intermolecular N–H···O interactions. Thus, for even a small subset of thioamide derivatives it is clear that no dominent synthon exists, a conclusion consistent with the observations made by Allen *et al.* for many organic molecules.[2] A noteworthy feature of the three last mentioned structures is that the conformation about the central C–N bond is *Z*. This conformation is different to the earlier examples and so raises the question as to which conformation is indeed the most stable. In other words, do thiocarbamide structures have a preferential conformation, *E* or *Z*, or is the observed isomer dictated by crystal packing considerations that force a specific conformation in order to optimise intermolecular interactions. In this contribution, this question is probed employing crystallographic, NMR and theoretical investigations for a series of compounds with the general formula MeOC(=S)N(H)C_6H_4-4-Y: Y = H (**1**), NO_2 (**2**), C(=O)Me (**3**), Cl (**4**) and C(=O)OMe (**5**). The crystal structure of the parent compound (**1**) is known[11] and was originally prepared in connection with the development of insecticides.[17] The related species **2** and **4** were first prepared around the same time and investigated for herbicidal activity.[18]

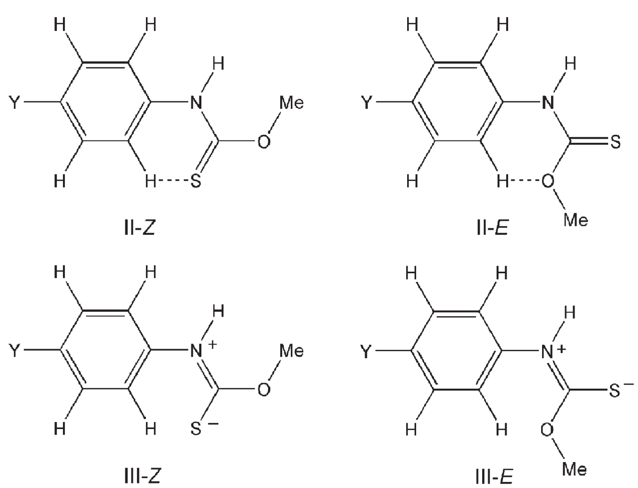

Chart 2 Intramolecular hydrogen-bonding (**II**) and resonance structures (**III**) for *O*-methyl-*N*-aryl-thiocarbamides.

Results and discussion

Solid-state structures

The molecular structures of MeOC(=S)N(H)C_6H_4-4-Y: Y = H (**1**),[11] NO_2 (**2**), C(=O)Me (**3**), Cl (**4**) and C(=O)OMe (**5**) are illustrated in Fig. 1.

Selected geometric parameters for all five molecules are collected in Table 1. The structure of **4** crystallises with two independent molecules in the crystallographic asymmetric unit. The overall conformations of the two molecules in **4** are very similar with the greatest differences between the molecules being manifested in the S1/C1/N1/C2 and O1/C1/N1/C2 torsion angles that differ by a few degrees. In each of **1–5** the central COC(=S)NC chromophore is essentially planar, and this planarity extends to include the aryl group in all but **1**. The molecules exist as a thione consistent with the adoption of the N–H tautomeric form, see structures **II–E** and **II–Z** in Chart 2. Nevertheless, there is significant delocalisation of π-electron density over the O–C(S)–N chromophore as evidenced by the bond distance data listed in Table 1. This observation, coupled with the planarity of this region of the molecule, allows assignment of *E*- and *Z*-conformations as discussed in the Introduction. The key difference between the five molecules is found in the structure of **5**, having a *Z*-conformation about the C1–N1 bond in contrast to the *E*-conformation found in the other structures. A common feature of the four structures having an *E*-conformation is the prevalence of a centrosymmetric {···H–N–C=S}$_2$ synthon; see Table 2 for geometric parameters associated with the hydrogen-bonding interactions operating in **1–5**. In **4**, the dimer formation occurs between pairs of independent molecules. In the crystal structures of **1–3**, the hydrogen-bonded dimers associate *via* O···H interactions to form tapes as illustrated in Fig. 2.

Thus, in **1**, centrosymmetrically related OMe groups associate (Table 2) *via* six-membered {···H–C–O}$_2$ rings ($R_2^2(6)$); Fig. 2a. Indeed, the hydrogen atom involved in this interaction may be considered as bifurcated as it also forms a close interaction with the phenyl ring so that C–H···π(C2–C7) is 2.87 Å and the angle subtended at H is 125°. The tapes associate *via* weak π···π interactions formed between centrosymmetrically related aromatic rings so that the separation between ring centroids is 3.831(1) Å (symmetry operation: $-x$, $-y$, $2 - z$). Owing to the twist around the N–C_{aryl} ring, these interactions occur to either side of the tape. Similar C–H···O contacts are observed in the crystal structure of **2** but this time occurring between one of the phenyl-H atoms and a nitrate oxygen atom so that ten-membered {···H–C–C–N–O}$_2$, ($R_2^2(10)$), rings are formed; Fig. 2b. Tapes associate into layers *via* weak π···π interactions (ring centroid distance: 3.850(1) Å for symmetry operation: $-x$, $-y$, $-z$). Successive layers stack along the *c*-axis, are rotated approximately ±50° to each other, and are associated *via* O···H interactions involving the second nitrate–oxygen atom which is bifurcated to two phenyl-H atoms. Unlike the structure of **1**, the methoxy-O atom does not form a significant intermolecular interaction but, owing to

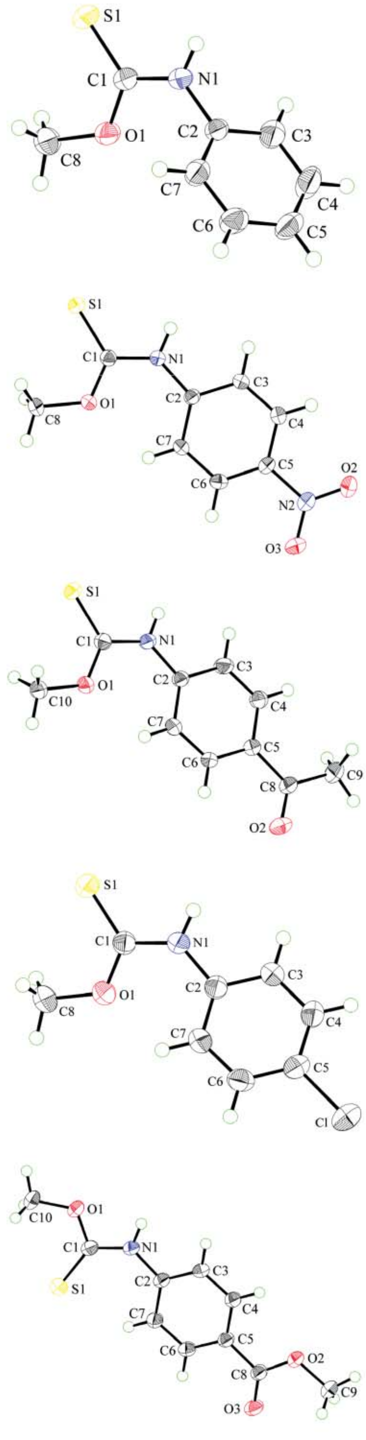

(1)

(2)

(3)

(4)

(5)

Fig. 1 Crystallographic numbering schemes for MeOC(=S)N(H)-C_6H_4-4-Y: (**1**) Y = H;[11] (**2**) Y = NO_2; (**3**) Y = C(=O)Me; (**4**) Y = Cl, the numbering scheme for the second independent molecule is as shown but with an added "a"; and (**5**) Y = C(=O)OMe.

its co-planarity with the aromatic ring, forms a tight intramolecular O···H_{phenyl} interaction of 2.42 Å. A similar $O_{methoxy}$···H_{phenyl} interaction of 2.19 Å exists in the structure of **3** in which the molecular tape features 22-membered {···H–C–O–C–N–C_5–O}$_2$ rings, $R_2^2(22)$, involving the carbonyl-O and methoxy-H atoms in addition to the {···H–N–C=S}$_2$ synthon. In **3**, the tapes, Fig. 2c, are held together by C–H···π

Table 1 Selected interatomic parameters (Å, °) for MeOC(=S)-N(H)C_6H_4-4-Y: Y = H (**1**),[1] NO_2 (**2**), C(=O)Me (**3**) Cl (**4**) and C(=O)OMe (**5**) derived from the X-ray crystallographic study and *ab initio* molecular orbital calculations (*in italics*)

Compound	**1**[11]	**2**	**3**	**4a**	**4b**	**5**
C1–S1	1.671(1)	1.664(2)	1.666(3)	1.656(2)	1.661(2)	1.647(2)
	1.67	*1.66*	*1.66*	*1.66*	*1.66*	*1.66*
C1–O1	1.329(1)	1.322(2)	1.317(3)	1.318(2)	1.322(2)	1.339(2)
	1.33	*1.32*	*1.32*	*1.33*	*1.33*	*1.32*
C1–N1	1.329(2)	1.345(2)	1.341(4)	1.335(2)	1.333(2)	1.347(2)
	1.35	*1.36*	*1.36*	*1.35*	*1.35*	*1.36*
N1–C2	1.431(1)	1.411(2)	1.409(4)	1.414(2)	1.410(2)	1.411(2)
	1.40	*1.39*	*1.40*	*1.40*	*1.40*	*1.40*
S1–C1–O1	124.5(1)	124.5(1)	124.6(2)	124.5(1)	124.5(1)	123.4(1)
	125.5	*126.0*	*125.7*	*125.6*	*125.6*	*125.7*
S1–C1–N1	123.0(1)	121.9(1)	121.8(2)	122.6(1)	122.8(1)	129.6(1)
	121.5	*121.2*	*121.3*	*121.4*	*121.4*	*121.3*
O1–C1–N1	112.5(1)	113.6(2)	113.6(2)	112.8(1)	112.7(1)	107.0(1)
	113.0	*112.9*	*112.9*	*112.9*	*112.9*	*113.0*
S1/C1/N1/C2	178.2(1)	−175.9(1)	174.8(3)	178.6(1)	−173.8(1)	−0.4(2)
O1/C1/N1/C2	−3.6(2)	5.3(2)	−6.4(5)	−2.7(2)	6.1(2)	178.6(1)
C1/N1/C2/C3	−60.1(2)	−176.0(2)	177.1(3)	161.4(2)	162.9(2)	−170.4(2)

Table 2 Geometric parameters associated with the hydrogen-bonding (A–H···B) in MeOC(=S)N(H)C_6H_4-4-Y: Y = NO_2 (**2**), C(O)Me (**3**), Cl (**4**) and C(O)OMe (**5**)

	A, B	H···B/Å	A···B/Å	A–H···B/°	Symmetry operation
1	N1, S1	2.51	3.359(1)	165	$-x, -y, 1-z$
	C8, O1	2.98	3.554(1)	127	$1-x, -1-y, 1-z$
2	N1, S1	2.56	3.412(2)	165	$1-x, 1-y, 1-z$
	C6, O3	2.61	3.508(2)	160	$-x, 1-y, -z$
	C3, O2	2.85	3.389(2)	118	$½-x, ½+y, -½-z$
	C4, O2	2.82	3.370(2)	118	$½-x, ½+y, -½-z$
3	N1, S1	2.55	3.406(3)	168	$1-x, 1-y, -1-z$
	C10, O2	2.48	3.287(4)	141	$-x, 1-y, -z$
4	N1, S1a	2.61	3.469(1)	169	$1-x, 1-y, 1-z$
	N1a, S1	2.54	3.397(1)	168	$1-x, 1-y, 1-z$
5	N1, O3	2.09	2.950(2)	171	$1+x, y, z$
	C3, O3	2.60	3.379(2)	141	$1+x, y, z$
	C6, O1	2.43	3.361(2)	169	$-1+x, y, z$
	C9, S1	3.01	3.617(2)	122	$-½+x, ½-y, -½+z$
	C9, S1	3.08	3.914(2)	145	$-x, -y, -z$

(H···ring centroid = 2.86 Å and angle at H = 136° for symmetry operation $1-x$, $2-y$, $-z$) and weak π···π interactions (3.976(2) Å for $1-x$, $1-y$, $-z$). While H-bonded tapes are not found in **4**, Cl···H interactions play a pivotal role in determining the global crystal structure as no evidence for significant π···π and C–H···π interactions was found. A layer structure is apparent in which layers comprising {···H–N–C=S}$_2$ synthons, connected laterally *via* Cl···H interactions, are linked to adjacent layers, also *via* Cl···H interactions, as the chloride atoms occupy positions exclusively at the surfaces of each layer. The closest Cl···H interaction involving the chloride atom of molecule *a* is 3.09 Å, involves a phenyl-H and serves to link layers, whereas for the chloride atom of molecule *b*, the shortest contact of 2.90 Å involves a methyl-H but also links two layers. A view of the unit cell contents for **4** is shown in Fig. 3.

Layers are also found in the structure of **5** but these are mediated by H-bonding interactions. The supramolecular association operating in the structure of **5** is illustrated in Fig. 4 and immediately apparent from this diagram is that the {···H–N–C=S}$_2$ synthons observed in the previous four

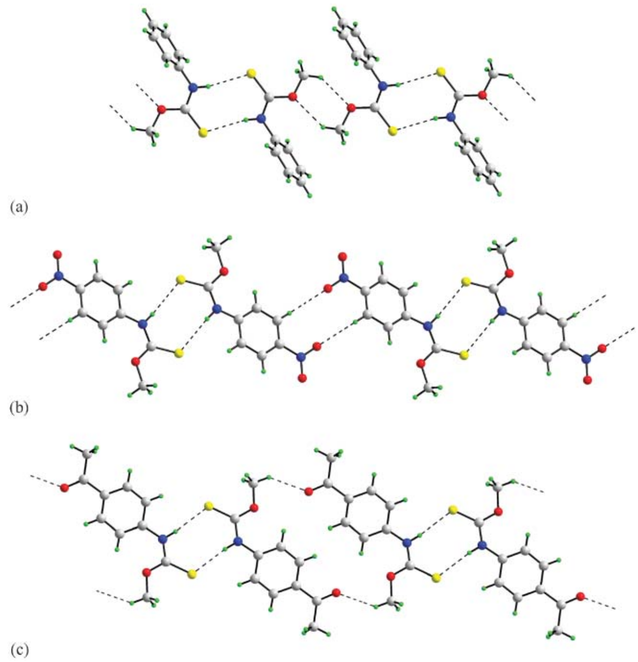

Fig. 2 Supramolecular association in MeOC(=S)N(H)C_6H_4-4-Y: (a) Y = H (**1**); (b) Y = NO_2 (**2**); (c) Y = C(=O)Me (**3**). Intramolecular C–H···O interactions are not shown for reasons for clarity. Click here to access a 3-D rotatable image of Fig. 2b. Click here to access a 3-D rotatable image of Fig. 2c.

structures are absent and that the conformation about the central C–N bond is now *Z*. Discernible tapes are evident which are formed *via* nine-membered {···H–N–C–O···H–C_3–O} rings occurring between translationally related molecules

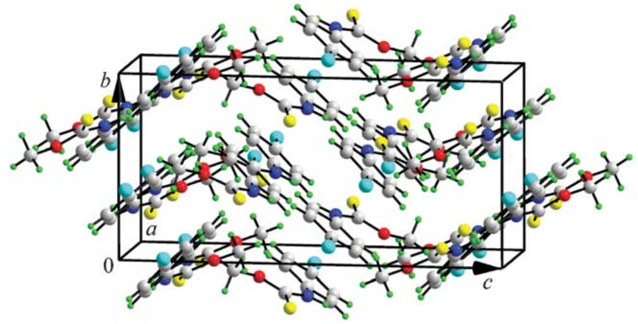

Fig. 3 Unit cell contents viewed for (**4**). Click here to access a 3-D rotatable image of Fig. 3.

having a head-to-tail arrangement. The $R_2^2(9)$ rings involve the amide-H and ester carbonyl atoms. Translationally related tapes are linked *via* S···H_{methyl} contacts so that a layer structure, stacked along the *b*-direction, is formed that has an undulating topology, as shown in the second view of Fig. 4. The primary interactions between successive layers again involve S···H_{methyl} contacts, there being no π···π and C–H···π interactions of note.

In conclusion, the crystallographic studies reported previously[11–16] and here, have shown that the {···H–N–C=S}$_2$ synthon does not predominate in the crystal structures of molecules with the general formula, MeOC(=S)N(H)R′, and in the same way, both *E*- and *Z*- conformations about the central C–N bond may be found. Clearly, there is an interplay between the adoption of an *E*-conformation and the formation of the {···H–N–C=S}$_2$ synthon on the one hand, and the adoption of a *Z*-conformation and some other supramolecular synthon on the other. The question then arises: what is the

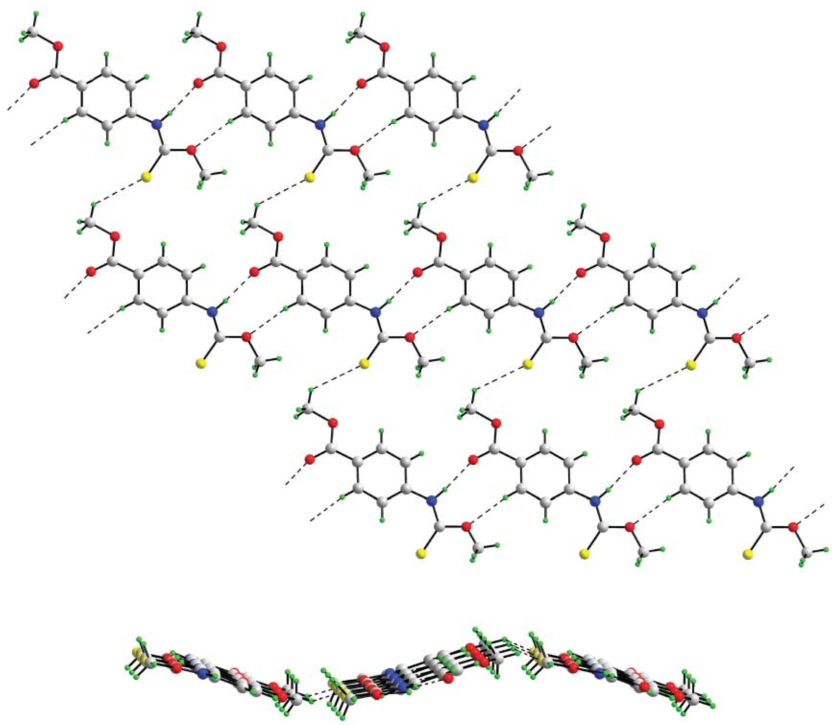

Fig. 4 Supramolecular association in MeOC(=S)N(H)C_6H_4-4-C(=O)OMe (**5**).

factor that is dictating the adoption of the isomeric conformation, *i.e.* *E*- or *Z*-, in MeOC(=S)N(H)R′. In other words, is the conformation determined by electronic effects associated with the *R*′ substitutent, or is the solid-state conformation determined by crystal packing considerations. In order to address these considerations, both experimental (*i.e.* solution NMR) and theoretical (molecular orbital calculations) studies were conducted for **1–5**.

Solution-state structures

Variable temperature ^{1}H NMR data for **1–5** recorded in CD_2Cl_2 solution are listed in Table 3. At 20 °C, each compound displays a pattern of resonances consistent with one species only. However, upon cooling, splitting in some resonances is evident. Typically, for **1**, the well-defined but broad resonance at 4.08 ppm due to OCH_3 at 20 °C begins to split at 0 °C and appears as two distinct resonances at lower temperatures. Similarly, the resonance assigned to the N–H nucleus appears as a broad resonance at 8.44 ppm at 20 °C but is split at lower temperatures. The aromatic protons appear as two doublets, one sharp and one somewhat broader. On cooling, both doublet resonances split into two sets of doublets. These observations are consistent with the presence of an exchange equilibrium between two species, which is rapid at room temperature but slows on cooling. The coalescence temperature for compounds **1–5** is between −20 and +20 °C.

By comparisons with similar systems[19,20] the two species observed at reduced temperatures are assigned as *E*- and *Z*-conformers. The more shielded resonances for N–H and OCH_3 for each of **1–5** are due to the minor component, which is assigned as the *Z*-isomer. The observation that the aromatic *ortho*-protons of the minor species are more deshielded is consistent with this assignment.[19] At the lowest temperature attained in the experiments, based on the integration of the resonances ascribed to OCH_3, the major isomer was present in the range from 83 to 90%.

As expected, there are small upfield shifts in the OCH_3 resonances with decreasing temperature. After being resolved at −20 °C, there is a small downfield shift for N–H due to the *Z*-isomer as the temperature is lowered. By contrast, for N–H due to the *E*-isomer, a downfield shift of more than 1 ppm is noted with decreasing temperature. The explanation for these solution phenomena is based on hydrogen-bonding considerations. The *E*-isomer can co-operatively form hydrogen bonds to form dimers mediated by two N–H···S interactions. On the other hand, dimers formed by the *Z*-isomer, with association moderated by only one N–H···S interaction as well as, presumably, C–H···O interactions, akin to that shown in the crystal structure of **5**, would occur. Based on the above, it is assumed that the *E*-isomer is stabilised in solution with respect to the *Z*-isomer and that as hydrogen-bonding considerations become more significant, *i.e.* at lower temperature, the *E*-isomer predominates further. Supporting this conclusion is the significant downfield shift associated with the N–H atom of the *E*-isomer but not that of the *Z*-isomer.

Dilution studies on **5** at −80 °C in CD_2Cl_2 show that the N–H proton resonances become more deshielded with increasing concentration, indicative of increased hydrogen bonding. A ROESY experiment on compound **5** at −80 °C in CD_2Cl_2 confirmed through space interaction between the N–H proton and the two aromatic *ortho*-protons for both the major and minor species.

To substantiate the importance of hydrogen bonding, spectra of **5** were recorded in CH_3OD, a solvent which is likely to minimise the intermolecular hydrogen-bonding association. The methoxy-proton at 4.12 ppm at 20 °C splits into two resonances of equal intensity at −40 °C. Apparently, in these circumstances there is no appreciable energy difference between *E*- and *Z*-conformations.

While it is assumed that the predominant isomer in dichloromethane solution is the same for each of **1–5**, based on the similarity of the spectra, and that the conformation of this is *E*-, definitive evidence is lacking, however. Accordingly, the molecules were subjected to molecular orbital calculations in order to gain insight into the relative stabilities of the various isomers that can exist for each of **1–5**.

Theoretical structures

Unconstrained geometry optimisation calculations were performed for **1–5** using DFT at the B3LYP/6-311G(2*df*,2*pd*) level of theory with the GAUSSIAN 98 suite of programs[21] using both *E*- and *Z*-conformations as starting points. In the case of **4**, for which two independent molecules comprise the crystallographic asymmetric unit, both converged to the same

Table 3 Selected variable temperature ^{1}H NMR data (δ, ppm) recorded in CD_2Cl_2 solution for MeOC(=S)N(H)C_6H_4-Y-4: Y = H (**1**),[1] Y = NO_2 (**2**), Y = C(=O)Me (**3**) Y = Cl (**4**), and Y = C(=O)OMe (**5**)

Compound, Temp./°C	*E*-N–H	*Z*-N–H	*E*-C(=S)OMe (%)	*Z*-C(=S)OMe (%)	C(=O)Me^A/C(=O)OMe^B
1, 20	8.44 s, br	8.44 s, br	4.08 s	4.08 s	
1, 0	8.61 s	8.07 s	4.10 s, br	4.01 s, br	
1, −20	8.80 s	8.10 s	4.09 s (70)	3.99 s (30)	
1, −40	9.07 s	8.15 s	4.08 s (83)	3.97 s (17)	
1, −60	9.43 s	8.20 s	4.07 s (86)	3.96 s (14)	
1, −80	9.83 s	8.25 s	4.05 s (88)	3.94 s (12)	
2, 20	8.21 s, br	8.21 s, br	4.14 s	4.14 s	
2, −80	9.19 s	8.53 s	4.14 s (83)	3.96 s (17)	
3, 20	8.44 s, br	8.44 s, br	4.12 s	4.12 s	2.53 s^A
3, −80	9.59 s	8.87 s	4.11 s (89)	3.93 s (11)	2.53 s^A
4, 20	8.29 s, br	8.29 s, br	4.07 s	4.07 s	
4, −80	9.56 s	8.18 s	4.06 s (83)	3.93 s (17)	
5, 20	8.44 s, br	8.44 s, br	4.12 s	4.12 s	3.86 s^B
5, −80	9.68 s	8.75 s	4.11 s (90)	3.92 s (10)	3.79 s^B

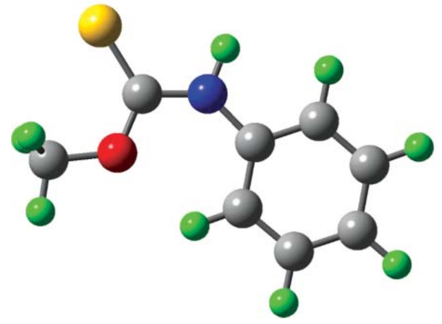

Fig. 5 Geometry optimised structure for MeOC(=S)N(H)C_6H_5 (**1**).

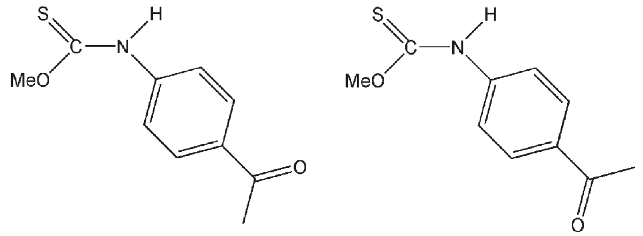

Chart 3 Alternate conformations of the –C(=O)Me group in **3**.

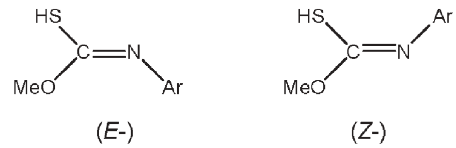

Chart 4 *E*- and *Z*-conformers for tautomeric forms of MeOC(=S)N(H)C_6H_4-4-Y.

energy-minimised structure. As a general principle, in the absence of crystal packing considerations, each molecule was of higher (mirror) symmetry and all non-hydrogen atoms were co-planar. The mirror symmetry is particularly noteworthy in the optimised strucutre of **1** for which a non-planar conformation was found in the solid state; the geometry optimised strucutre is shown in Fig. 5.

This symmetrisation of the structures matches that found in our related work on organotin systems.[22–26] As summarised in Table 4, the global energy-minimised structure in each case had the *E*-conformation. When analogous calculations were performed assuming a matrix of solvent, *i.e.* using an Isodensity Polarised Continum (overlapping spheres) Model, the same results were obtained but the differences in energies between the *E*- and *Z*- isomers were reduced a little. In the cases of **3** and **5**, where alternate conformations can be envisaged for the Y group with respect to the rest of the molecule, *i.e.* C(=O)Me, see Chart 3, and C(=O)OMe, the differences in energies were calculated to be less than 0.21 kJ mol^{-1}, indicating a minimal influence. Finally, as a representative example, geometry optimisations for **1** were performed assuming that the molecules existed as tautomers as shown in Chart 4. For the *E*- and *Z*-conformations, these are at least 70 kJ mol^{-1} more energetic than the most stable *E*-isomer.

The geometric parameters derived from the theoretical study for the most stable *E*-isomer of **1–5** are included (*in italics*) in Table 1. There is a close match between the experimental and theoretical values for **1–4**, inspiring confidence in the calculations, and supporting the conclusions of the X-ray study, in particular the additional electron density in the central C–N bond that allows the *E*- *vs*. *Z*-nomenclature to be adopted.

Table 4 Selected thermodynamic data (kJ mol^{-1}) derived from the theoretical study of MeOC(=S)N(H)C_6H_4-Y-4: Y = H (**1**), Y = NO_2 (**2**), Y = C(=O)Me (**3**) Y = Cl (**4**), and Y = C(=O)OMe (**5**)

	ΔH ($E - Z$)	ΔH($E - Z$)[a]	S[b]	O[b]	N[b]	H[b]
1	4.95	2.69	−0.37	−0.33	−0.32	0.14
2	4.01	2.16	−0.33	−0.33	−0.33	0.14
3	4.07	3.11	−0.35	−0.33	−0.33	0.14
4	4.76	3.92	−0.36	−0.33	−0.33	0.14
5	5.36	3.39	−0.35	−0.33	−0.33	0.14

[a] Assuming a matrix of CH_2Cl_2 solvent (see text). [b] Mulliken population charge analysis of the atoms in the {H–N–C=S}$_2$ synthon.

Differences noted between the experimental and theoretical parameters for **5** are directly related to the adoption of a different conformation in the solid-state compared with the optimised geometry. In terms of the geometric parameters obtained from the theoretical calculations alone, these basically show invariance as the nature of Y varies. Indeed, the greatest differences in the geometric parameters are related to the S1/C1/N1/C2, O1/C1/N1/C2 and C1/N1/C2/C3 torsion angles that are all 0° in the optimised structures owing to the above-mentioned co-planarity of the non-hydrogen atoms. The invariance in the geometric parameters as Y varies is borne out in the values obtained from the Mulliken population analysis; see data in Table 4. These results show a uniform distribution of charge over the atoms comprising the central chromophore and thereby precludes an electronic argument as being the reason for the adoption of one conformation over the other.

Summary and conclusions

Crystallography shows that compounds **1–4** crystallise with an *E*-conformation about the central C–N bond that faciliates the formation of centrosymmetric {···H–N–C=S}$_2$ hydrogen-bonded rings. These rings are linked into tapes *via* C–H···O interactions for **1–3**; in **4**, a cohesive crystal lattice is stabilised by C–H···Cl interactions. By contrast, the structure of **5** adopts a *Z*-conformation and {···H–N–C–O···H–C_3–O} rings are the predominant synthon, linked again *via* C–H···O and C–H···S interactions into a layer structure. In solution, based on variable-temperature ^{1}H NMR measurements, both *E*- and *Z*-conformations co-exist with the former dominant, particularly at lower temperature as a result of hydrogen-bonding considerations. Theoretical studies indicate that for each of **1–5**, the *E*-conformation is the more stable by about 5 kJ mol^{-1}; both *E*- and *Z*-isomers are significantly more stable than their corresponding S–H tautomeric forms. The calculated energy differences are in the realm of the energy of stabilisation for crystal structures of organic molecules, *i.e.* 4–8 kJ mol^{-1}.[27]

With such relatively small energy differences between the *E*- and *Z*-conformations for **1–5**, it is perhaps not surprising that the ultimate isomer found in the solid state is dictated by crystal packing in certain circumstances. Thus, while there is experimental and theoretical evidence to indicate that the *E*-conformation is the more stable form for molecules **1–5**, this preference is overwhelmed by global crystal packing considerations that favour the adoption of a *Z*-conformation for **5**.

Experimental

Preparation of MeOC(=S)N(H)Ar

The ligands were prepared in a similar manner to the literature procedure.[17] The aryl isothiocyanate (Lancaster) was added dropwise to a stirred solution of KOH (1 mol equiv) in MeOH (25 ml) that also functioned as the solvent. Excess HCl (3 M) was added dropwise to this solution, producing an oily suspension that was left to stir for 1 h; the product was then extracted from the aqueous solution with $CHCl_3$. The product was isolated by recrystallisation from a $CHCl_3$ solution of the compound that had been layered with hexane.

Infrared data were recorded as KBr discs on a Excalibur Series Bio-Rad Merlin FTS 3000 spectrophotometer. Generally, ^1H and $^{13}C\{^1H\}$ NMR data ($CDCl_3$) were measured on a Bruker ACF 300 MHz FT spectrometer operating at 300.13 and 75.44 MHz, respectively, using TMS as the internal reference. $^{13}C\{^1H\}$ NMR data ($CDCl_3$) for **3** and **5** were measured on a Bruker ACF 500 MHz FT spectrometer operating at 125.72 MHz. The ROESY (Rotating frame Overhauser Enhancement SpectroscopY) spectrum of **5** was obtained using a JEOL Eclipse Plus 400 spectrometer with the standard ROESY pulse sequence, a spin lock time of 0.7 s and a spin lock attenuation of 12 dB. Microanalytical data were measured on a Perkin-Elmer PE 2400 CHN Elemental Analyzer for dried samples.

MeOC(=S)N(H)Ph (**1**) Obs. (Calc.): C, 57.6 (57.5); H, 5.5 (5.4); N, 8.5 (8.4); S, 20.5 (19.1). IR (KBr, cm^{-1}): 3241(br) ν(N–H), 1447(s) ν(C–N), 1207(m) ν(C=S), 1058(m) ν(C–O). NMR ($CDCl_3$): ^{13}C δ 189.5 (Cq), 137.1 (Ph, C1), 129.0 (Ph, C3), 125.6 (Ph, C2), 121.9 (Ph, C4), 58.7 (OCH_3). Mp 92–94 °C.

MeOC(=S)N(H)C_6H_4-4–NO_2 (**2**) Obs. (Calc.): C, 45.0 (45.3); H, 3.6 (3.8); N, 12.7 (13.20); S, 15.5 (15.1). IR (KBr, cm^{-1}): 3236 (br) ν(N–H), 1456(s) ν(C–N), 1207(s) ν(C=S), 1039(s) ν(C–O). NMR ($CDCl_3$): ^{13}C δ 189.0 (Cq), 142.7 (Ph, C1), 130.7 (Ph, C4), 125.0 (Ph, C2), 120.5 (Ph, C3), 58.7 (OCH_3). Mp 188–189 °C.

MeOC(=S)N(H)C_6H_4-4–C(=O)Me (**3**) Obs. (Calc.): C, 57.4 (57.8); H, 5.3 (5.2); N, 6.7 (6.7); S, 15.3 (15.2). IR (KBr, cm^{-1}): 3229 (br) ν(N–H), 1460(m) ν(C–N), 1221(m) ν(C=S), 1047(m) ν(C–O). NMR ($CDCl_3$): ^{13}C δ 196.8 (C(O)Me), 189.2 (Cq), 141.2 (Ph, C1), 133.6 (Ph, C4), 129.6 (Ph, C3), 120.6 (Ph, C2), 58.4 (OCH_3), 26.4 (C(O)CH_3). Mp 118–119 °C.

MeOC(=S)N(H)C_6H_4-4–Cl (**4**) Obs. (Calc.): C, 47.7 (47.8); H, 4.0 (3.9); N, 7.0 (6.9); S, 15.9 (15.9). IR (KBr, cm^{-1}): 3236(br) ν(N–H), 1456(s) ν(C–N), 1449(m) ν(C–N), 1042(m) ν(C–O). NMR ($CDCl_3$): ^{13}C δ 189.4 (Cq), 135.6 (Ph, C1), 130.9 (Ph, C4), 129.1 (Ph, C3), 123.0 (Ph, C2), 58.9 (OCH_3). Mp 94–96 °C.

MeOC(=S)N(H)C_6H_4-4–C(=O)OMe (**5**) Obs. (Calc.): C, 53.6 (53.8); H, 4.4 (4.9); N, 7.4 (6.2); S, 14.1 (14.2). IR (KBr, cm^{-1}): 3247(br) ν(N–H), 1460 m ν(C–N), 1220 m ν(C=S), 1049 m ν(C–O). NMR ($CDCl_3$): ^{13}C δ 189.2 (Cq), 166.4 (*C*(=O)OMe), 141.1 (Ph, C1), 130.7 (Ph, C3), 126.4 (Ph, C4), 120.5 (Ph, C2), 58.5 (OCH_3), 52.1 (C(=O)OCH_3). Mp 132–133 °C.

Computational details

Geometries: All geometric optimisation and frequency calculations for **1–5** were performed with the GAUSSIAN 98 suite of programs[21] using DFT at the B3LYP/6-311G(2*df*,2*pd*) level of theory. The starting points for the calculations were generated using the crystallographically determined coordinates and

Table 5 Crystallographic data and refinement details for MeOC(=S)N(H)C_6H_4-Y-4: Y = NO_2 (**2**), Y = C(=O)Me (**3**) Y = Cl (**4**), and Y = C(=O)OMe (**5**)

Compound	2	3	4	5
Formula	$C_8H_8N_2O_3S$	$C_{10}H_{11}NO_2S$	C_8H_8ClNOS	$C_{10}H_{11}NO_3S$
M	212.22	209.26	201.66	225.26
Crystal system	Monoclinic	Triclinic	Monoclinic	Monoclinic
Space group	$P2_1/n$	$P\bar{1}$	$P2_1/n$	$P2_1/n$
a/Å	7.3340(6)	5.6059(8)	14.5243(10)	8.1538(9)
b/Å	7.6604(6)	7.9101(11)	7.7142(6)	6.8174(8)
c/Å	16.1964(11)	11.9617(13)	17.2760(12)	18.976(2)
α/°	90	99.223(3)	90	90
β/°	95.632(2)	101.517(3)	110.560(2)	97.586(3)
γ/°	90	100.210(4)	90	90
V/Å^3	905.54(12)	500.87(11)	1812.4(2)	1045.6(2)
Z	4	2	8	4
D_x/g cm^{-3}	1.557	1.388	1.478	1.431
Crystal size/mm	0.13 × 0.16 × 0.29	0.07 × 0.26 × 0.39	0.12 × 0.17 × 0.34	0.04 × 0.23 × 0.39
μ/mm^{-1}	0.338	0.295	0.600	0.295
Independent reflections	2631	2861	5300	3036
Observed reflections ($I \geqslant 2\sigma(I)$)	2090	2264	3831	2043
$R(F^2)$ (observed reflections)	0.049	0.069	0.043	0.047
a and b for weighting scheme	0.058; 0.302	0.112; 0.258	0.066; 0	0.076; 0
$wR(F^2)$ (all data)	0.122	0.221	0.121	0.125
ρ/e Å^{-3}	0.49	0.51	0.50	0.48

optimised without any assumptions. In order to help elucidate the most stable isomer, other initial conformations were generated by rotating about the central C–N bond as well as about the C–Y bond of the aromatic ring and again allowed to optimise without constraints. Frequency calculations were performed for all the optimized structures in order to confirm that they were indeed true minima.

Energies: The $\Delta_r G^0$ reported in Table 4 for the gas phase were computed at 298.15 K and 1 atm using the harmonic frequencies (unscaled). For the values in solution, the Isodensity Polarised Continum (overlapping spheres) Model (IPCM), implemented in a Self-Consistent Reaction Field method in GAUSSIAN 98,[21] was used at the minima obtained in the gas-phase. The difference in the solvation-free energies was subtracted from the gas-phase $\Delta_r G^0$ to obtain the solution phase $\Delta_r G^0$.

Crystallography

Intensity data were measured at 223(2) K on a Bruker SMART CCD diffractometer employing Mo Kα radiation. Data processing and absorption correction were accomplished with SAINT[28] and SADABS,[29] respectively. The structures were solved by heavy-atom methods[30] and refinement (anisotropic displacement parameters, hydrogen atoms in the riding model approximation and a weighting scheme of the form $w = 1/[\sigma^2(F_o^2) + (aP)^2 + bP]$ for $P = (F_o^2 + 2F_c^2)/3$) was on F^2.[31] Crystallographic data and final refinement details are given in Table 5. Fig. 1 was drawn with ORTEP[32] at the 50% probability level, Figs. 2–4 were drawn with the DIAMOND programme,[33] and that of Fig. 5 was drawn with the graphics software of Gaussian.[21] Data manipulation was with teXsan.[34]

CCDC reference numbers 262600–262603. For crystallographic data in CIF or other electronic format see DOI: 10.1039/b514254g

Acknowledgement

The University of Singapore is thanked for grants (R-143-000-213-112 & R-143-000-189-112) in support of this research.

References

1 M. C. Etter, J. C. MacDonald and J. Bernstein, *Acta Crystallogr.*, 1990, **B46**, 246.
2 F. H. Allen, W. D. S. Motherwell, P. R. Raithby, G. P. Shields and R. Taylor, *New J. Chem.*, 1999, 25.
3 R. Bardi, A. Del Pra, A. M. Piazzesi, L. Sindellari and B. Zarli, *Inorg. Chim. Acta*, 1981, **47**, 231.
4 U. Casellato, G. Fracasso, R. Graziani, L. Sindellari, A. Sánchez González and M. Nicolini, *Inorg. Chim. Acta*, 1990, **167**, 21.
5 P. Porta, *J. Chem. Soc. A*, 1971, 1217.
6 V. J. Hall, G. Siasios and E. R. T. Tiekink, *Aust. J. Chem.*, 1993, **46**, 561.
7 R. Rossi, A. Marchi, A. Duatti, L. Magon, U. Cassellato and R. Graziani, *J. Chem. Soc., Dalton Trans.*, 1988, 1857.
8 R. Rossi, A. Marchi, S. Aggio, L. Magon, A. Duatti, U. Cassellato and R. Graziani, *J. Chem. Soc., Dalton Trans.*, 1990, 477.
9 S. P. Abraham, N. Narasimhamurthy, M. Nethaji and A. G. Samuelson, *Inorg. Chem.*, 1993, **32**, 1739.
10 N. Narasimhamurthy, A. G. Samuelson and H. Manohar, *Chem. Commun.*, 1989, 1803.
11 S. Y. Ho, C. S. Lai and E. R. T. Tiekink, *Acta Crystallogr.*, 2003, **E59**, o1155.
12 R. Taylor and E. R. T. Tiekink, *Z. Kristallogr.*, 1994, **209**, 64.
13 S. P. Abraham, A. G. Samuelson and M. Nethaji, *Proc. Indian Acad. Sci., Chem. Sci.*, 1995, **107**, 255.
14 A. D. Morales, H. Novoa de Armas, N. M. Blaton, O. M. Peeters, C. J. De Ranter, H. Márquez and R. P. Hernández, *Acta Crystallogr.*, 2000, **C56**, 1042.
15 S. Zhang, Z. Wang, M. Li, K. Jiao, I. A. Razak, S. S. S. Raj and H.-K. Fun, *Acta Crystallogr.*, 2001, **C57**, 566.
16 G. Bernardinelli, T. Berclaz, M. Geoffroy and N. Rajalakshmi, *Acta Crystallogr.*, 1995, **C51**, 1390.
17 F. W. Plapp, Jr and T. M. Valega, *J. Econ. Entomol.*, 1967, **60**, 1094.
18 J. Myska, M. Smazik, A. Libicky, J. Stanek and J. Zemanek, *Collect. Czech. Chem. Commun.*, 1968, **33**, 4411.
19 A. Lindén and J. Sandström, *Acta Chem. Scand.*, 1973, **27**, 2567.
20 S. El Migirab, J. Jadot, P. Laszlo and A. Stockis, *Org. Magn. Reson.*, 1976, **8**, 115.
21 Gaussian 98. Revision A.7: M. J. Frisch, G. W. Trucks, H. B. Schlegel, G. E. Scuseria, M. A. Robb, J. R. Cheeseman, V. G. Zakrzewski, Jr., J. A. Montgomery, R. E. Stratmann, J. C. Burant, S. Dapprich, J. M. Millam, A. D. Daniels, K. N. Kudin, M. C. Strain, O. Farkas, J. Tomasi, V. Barone, M. Cossi, R. Cammi, B. Mennucci, C. Pomelli, C. Adamo, S. Clifford, J. Ochterski, G. A. Petersson, P. Y. Ayala, Q. Cui, K. Morokuma, D. K. Malick, A. D. Rabuck, K. Raghavachari, J. B. Foresman, J. Cioslowski, J. V. Ortiz, A. G. Baboul, B. B. Stefanov, G. Liu, A. Liashenko, P. Piskorz, I. Komaromi, R. Gomperts, R. L. Martin, D. J. Fox, T. Keith, M. A. Al-Laham, C. Y. Peng, A. Nanayakkara, C. Gonzalez, M. Challacombe, P. M. W. Gill, B. Johnson, W. Chen, M. W. Wong, J. L. Andres, C. Gonzalez, M. Head-Gordon, E. S. Replogle and J. A. Pople, Gaussian, Inc., Pittsburgh PA, 1998.
22 M. A. Buntine, V. J. Hall, F. J. Kosovel and E. R. T. Tiekink, *J. Phys. Chem. A*, 1998, **102**, 2472.
23 E. R. T. Tiekink, V. J. Hall and M. A. Buntine, *Z. Kristallogr.*, 1999, **214**, 124.
24 E. R. T. Tiekink, V. J. Hall, M. A. Buntine and J. Hook, *Z. Kristallogr.*, 2000, **215**, 23.
25 M. I. Mohamed-Ibrahim, S. See Chee, M. A. Buntine, M. J. Cox and E. R. T. Tiekink, *Organometallics*, 2000, **19**, 5410.
26 M. A. Buntine, F. J. Kosovel and E. R. T. Tiekink, *CrystEngComm*, 2003, **5**, 331.
27 J. P. Glusker, M. Lewis and M. Rossi, *Crystal Structure Analysis for Chemists and Biologists*, VCH, New York, 1994.
28 SAINT. Version V5.6. Bruker AXS Inc., Madison, WI.
29 SADABS. (*a*) G. M. Sheldrick, University of Gottingen, 2000; (*b*) R. Blessing, *Acta Crystallogr., Sect. A*, 1995, **51**, 33.
30 P. T. Beurskens, G. Admiraal, G. Beurskens, W. P. Bosman, S. García-Granda, J. M. M. Smits and C. Smykalla, *The DIRDIF program system, Technical report of the Crystallography Laboratory*, University of Nijmegen, 1992.
31 G. M. Sheldrick, SHELXL97, Program for the Refinement of Crystal Structures. University of Göttingen, 1997.
32 C. K. Johnson, ORTEP II, Report ORNL-5136, Oak Ridge National Laboratory, Oak Ridge, TN, 1976.
33 DIAMOND, Visual Crystal Structure Information System, Version 2.1e, CRYSTAL IMPACT, Postfach 1251, D-53002 Bonn, Germany, 2002.
34 teXsan, Structure Analysis Package, Molecular Structure Corporation, Houston, TX, 1992.